Available online at www.sciencedirect.com
SCIENCE DIRECT
Journal of African Earth Sciences 44 (2006) 561–570
Journal of African Earth Sciences
www.elsevier.com/locate/jafrearsci

Tectonic significance of Late Neoproterozoic granites from the Tibesti massif in southern Libya inferred from Sr and Nd isotopes and U–Pb zircon data

Ismail B. Suayah [1], Jonathan S. Miller [2], Brent V. Miller [3], Tovah M. Bayer [4], John J.W. Rogers [*,1]

Department of Geological Sciences, University of North Carolina, Chapel Hill, NC 27599–3315, United States

Received 1 September 2005; received in revised form 20 October 2005; accepted 3 November 2005
Available online 18 January 2006

Abstract

The Neoproterozoic crust of the Tibesti massif was stabilized by magmatism that included subduction-generated batholithic suites and post-orogenic granite plutons. All of the magmatism occurred in a period of about 20 million years centered around 550 Ma, and nearly all of the granites have initial $^{87}Sr/^{86}Sr$ ratios of about 0.706. The Wadi Yebigue pluton has U–Pb zircon ages of 563 Ma and 558 Ma on two different phases and ε_{Nd} at 550 Ma from −0.5 to −2.2. These isotopic data and the geologic history of the massif suggest that granites in the Tibesti massif developed during and shortly after closure of a short-lived ocean basin that developed by fragmentation of pre-existing continental crust of the Saharan region.

Keywords: Tibesti; Neoproterozoic; Sr isotopes; Nd isotopes; Zircon dating; Confined orogen

1. Introduction

The area shown in Fig. 1A is an arid region where rocks of Neoproterozoic and older age are almost completely covered by Phanerozoic sediments and desert sands. The lack of exposure throughout the region has led some geologists to refer to the region from the Arabian–Nubian shield to the West African craton by terms such as the "East Sahara Craton" or "Central Saharan Ghost Craton," and Abdelsalam et al. (2002) refer to much of the area as the "Saharan Metacraton."

This paper summarizes the limited isotopic information available from the Tibesti massif of southern Libya and northern Chad. It presents new information on the Wadi Yebique granite (Suayah and Rogers, 1986) and reviews older data from the Ben Ghnema batholith (Ghuma and Rogers, 1978) and young granites from Jebel Eghei (El Makhrouf and Fullagar, 2000).

2. Regional geology of North Africa

In order to compare the Tibesti massif (next section) with other parts of North Africa, we briefly summarize the general geology of North Africa and isotopic characteristics of rock suites from the Nubian–Arabian shield toward the west. More complete information and references are provided by Abdelsalam et al. (2002).

* Corresponding author.
E-mail address: jrogers@email.unc.edu (J.J.W. Rogers).
[1] Present address: TIBCO Extensibility, Inc, 200 W. Franklin Street, Suite 200, Chapel Hill, NC 27516, USA.
[2] Department of Geology, San Jose State University, San Jose, CA 95192-0102, USA.
[3] Present address: Department of Geology and Geophysics, Texas A&M University, College Station, TX 77843.
[4] Present address: Department of Geology, Western Washington University, Bellingham, WA 98225.

1464-343X/$ - see front matter © 2005 Elsevier Ltd. All rights reserved.
doi:10.1016/j.jafrearsci.2005.11.020

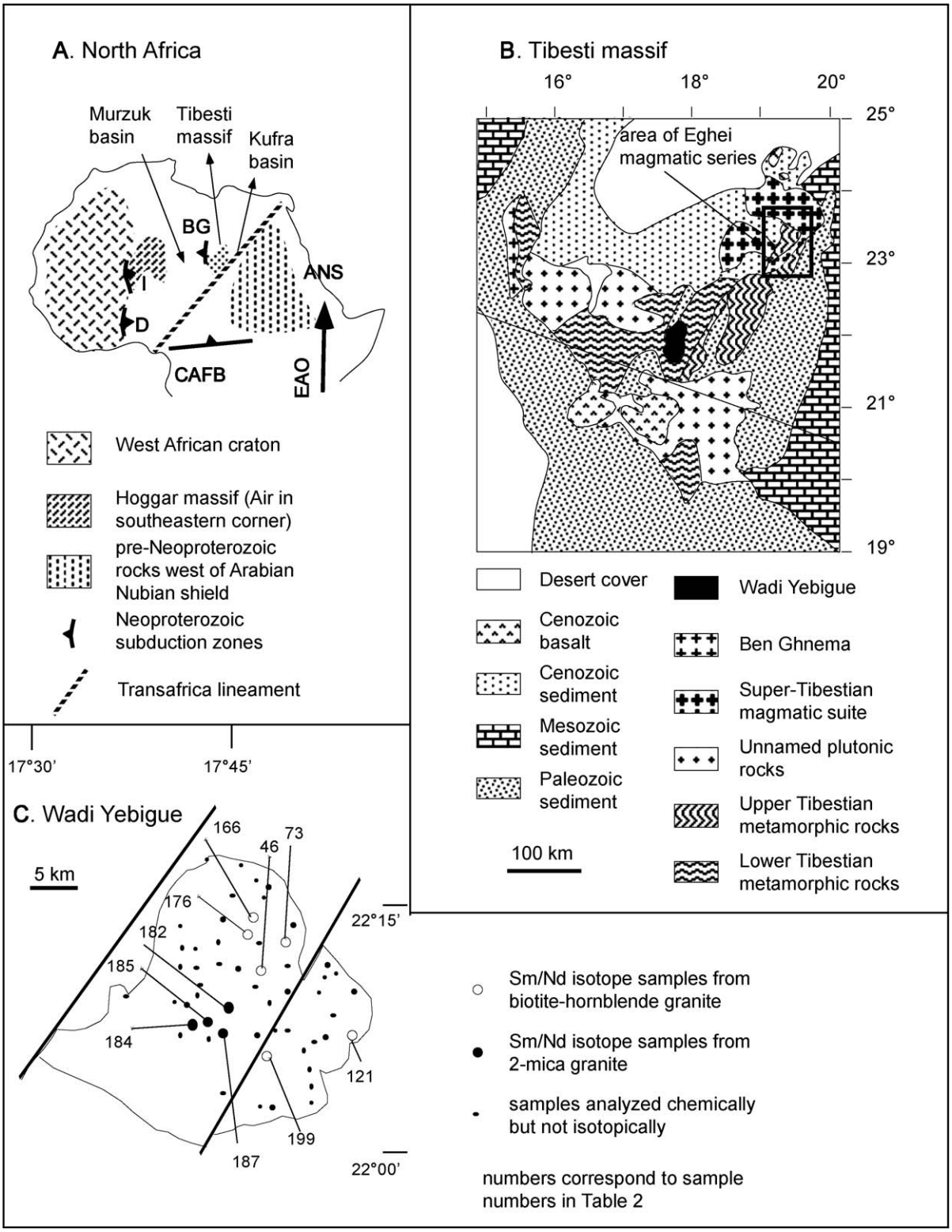

Fig. 1. A. Areas of Precambrian basement exposure in North Africa between the Arabian–Nubian shield and the West African craton. ANS, Arabian–Nubian shield; EAO, East African orogen. Late Neoproterozoic subduction zones are: BG, Ben Ghnema; I, Iforas; D, Dahomeyides; CAFB, Central African Fold Belt. B. General geology of Tibesti massif (summarized from Wacrenier and Vincent, 1958; Ghuma and Rogers, 1978; Suayah and Rogers, 1986; El-Makhrouf, 1988). Small plutons of the Eghei magmatic series occur within the area labeled. Cenozoic volcanic cones are not shown. C. Wadi Yebigue pluton, showing sample locations.

The Arabian–Nubian shield is the northern end of the East-African orogen, which extends along the east coast of Africa and probably continued through Madagascar, southern India, and into East Antarctica during Neoproterozoic time (Stern, 1994, 2002; Muhongo, 1999; Muhongo et al., 2003). The shield crops out between older continental blocks both on the east (in the Arabian Peninsula) and on the west (in North Africa). Rocks along the eastern margin show complex relationships along structures aligned N-S (Al-Saleh and Boyle, 2001), but most of the shield consists of assembled island-arc terranes and intervening suture zones with a NE-SW trend (Vail, 1985; Abdelsalam and Stern, 1996). Individual terranes contain basaltic/andesitic flow and pyroclastic rocks intruded by dioritic to minor granitic plutons, which probably formed at the same time as metamorphism of the supracrustal rocks to greenschist and low-amphibolite facies. Suture zones between the arcs are melanges that contain dismembered ophiolite complexes and other oceanic rock suites.

The island arcs and associated batholiths formed from about 900 Ma to 550 Ma. They have initial $^{87}Sr/^{86}Sr$ ratios from 0.7019 to 0.7038, $\varepsilon_{Nd(CHUR)}$ values of +1.6 to +7.7, and T_{DM} values only slightly older than crystallization ages (ranges summarized from Duyverman et al., 1982; Stern and Hedge, 1985; Stern and Kroner, 1993; Stern, 2002). Incorporation of some amount of old continental crust or enriched upper mantle in a few suites, however, is indicated by a granite with U–Pb zircon inheritance as old as 1600 Ma and two granites with initial $^{207}Pb/^{204}Pb$ of 15.561 and 15.611 (Sultan et al., 1990). Numerous undeformed, postorogenic, granite plutons invade both arc terranes and suture zones (Greenberg, 1981). The ages of these undeformed plutons range mostly from about 600 to 550 Ma, apparently coinciding with the final suturing of the island-arc terranes. Initial $^{87}Sr/^{86}Sr$ ratios of ~0.701 to ~0.70 and positive $\varepsilon_{Nd(CHUR)}$ values in almost all of the undeformed granites show that the source of most of the magmas was a mantle-derived crustal underplate without any components from older sialic crust (summarized from Abdel-Fattah and Doig, 1987; Stern and Kroner, 1993; Moghazi, 1999).

The western edge of the Arabian–Nubian shield and East African orogen probably occur along one or more suture zones (Abdelsalam et al., 2002). Harms et al. (1990) summarized isotopic characteristics of scattered exposures in the eastern Sahara west of the Arabian–Nubian shield (west of the Nile). Rocks in the Uweinat massif are as old as Neoarchean, but most rocks in the region west of the Nile are Neoproterozoic. Initial $^{87}Sr/^{86}Sr$ ratios of granitic rocks of Late Neoproterozoic age range from 0.706 to 0.710; $\varepsilon_{Nd(CHUR)}$ values of 14 granitic rocks range from +4 to −8.8 at 580 Ma, with an average of −5.44; and T_{DM} ranges from 0.86 Ga to 1.8 Ga, with an average of 1.46 Ga. This eastern Sahara region is terminated on the west by the Trans Africa lineament (Fig. 1A; Nagy et al., 1976), which crosses Africa and is particularly deep beneath the Kufra basin. Basement west of the Tibestis is now covered by the extensive Murzuk basin, which consists entirely of shallow-water Phanerozoic sediments. The western margin of this basin is the Tuareg shield (Caby and Andreopoulos-Renaud, 1987; Caby, 2003; Caby and Monie, 2003), which may represent an outcrop of the crystalline rocks beneath the Murzuk basin or may be a different massif structurally separated from the Murzuk block.

The largest part of the Tuareg shield is the Hoggar massif, which contains a complex sequence of fault slices apparently assembled by right-lateral transpression during Late Neoproterozoic time (Caby et al., 1989; Boullier, 1991; Black et al., 1994). Crystalline parts of the massif range from Archean through the Mesoproterozoic and include mainly ortho- and paragneisses, with some blocks metamorphosed to granulite facies (Caby, 1996). The southern extension of the eastern Hoggar in Air is an assemblage of arc-type terranes mostly cratonised at approximately 700 Ma. Ages of granites in Air obtained by U–Pb zircon methods are in the range of 500–700 Ma, with some suites showing Early Proterozoic inheritance (Liegeois et al., 1994). Granitic suites in Air that are younger than 700 Ma have initial $^{87}Sr/^{86}Sr$ ratios from 0.704 to 0.713; $\varepsilon_{Nd(CHUR)}$ values from −2.9 to −22.8 at ages from 660 Ma to 600 Ma; and T_{DM} values from 0.86 Ga to 1.8 Ga (all values from Liegeois et al., 1994).

The western part of the Hoggar massif and the Adrar des Iforas in the southwestern part of the Tuareg shield contain materials formed in the Pharusian ocean basin that bordered the West African craton during Pan-African time. The ocean closed at ~600 Ma, when subduction of oceanic lithosphere formed the Trans-Saharan orogenic belt (Boullier, 1991; Caby and Monie, 2003), which includes the Iforas orogen (Dostal et al., 1994) and the Dahomeyides (Attoh et al., 1997).

The southern margin of the Saharan region in the west is the Central African Fold Belt (Oubanguides; Toteu et al., 2001, 2004). Deformation along the fold belt developed by sinistral transpression during the Late Neoproterozoic, when terranes to the north were thrust upon the Congo craton. In the east, the southern limit of the Saharan Metacraton may be one or more sutures, with at least one trending southwestward from the Arabian–Nubian shield (Schandelmeier et al., 1994).

3. Geology of Tibesti massif

The Tibesti massif is one of the world's least known areas (Fig. 1B; summary of isotopic data in Tables 1–3). Wacrenier and Vincent (1958) recognized a basement consisting of at least two metamorphosed supracrustal

Table 1
Strontium isotopic data for granitic rocks of Tibesti massif

Unit	Age in Ma	Initial $^{87}Sr/^{86}Sr$	Reference
Ben Ghnema			
Western part	550+/−11	0.7062+/−0.0004	Pegram et al. (1976)
Eastern part	586+/−27	0.7052+/−0.0066	Pegram et al. (1976)
Pegmatites	533+/−5	0.7065+/−0.0004	Pegram et al. (1976)
Super-Tibestian	560+/−4	0.70529+/−0.000009	El-Makhrouf (1988)
Wadi Yebigue			
hb-bi and bi granite	558+/−5	0.70640+/−0.00039	Suayah and Rogers (1986)
2-mica granite	548+/−12	0.70693+/−0.00219	Suayah and Rogers (1986)
Eghei granites			
A.M. Salah	552+/−3	0.70436+/−0.00047	El Makhrouf and Fullagar (2000)
Kangara	554+/−6	0.70530+/−0.00046	El Makhrouf and Fullagar (2000)
Kangara–Tushidi	528+/−7	0.70791+/−0.00054	El Makhrouf and Fullagar (2000)
Zouma	532+/−7	1.24265+/−0.19032	El-Makhrouf (1988)
Eghei rhyolites			
Eruptives	537+/−7	0.70650+/−0.00030	El Makhrouf and Fullagar (2000)
Dikes	559+/−35	0.70330+/−0.00882	El Makhrouf and Fullagar (2000)

Initial $^{87}Sr/^{86}Sr$ ratios are isochron intercepts of whole-rock data.

units. The older unit (Lower Tibestian) contains metasedimentary and metavolcanic rocks mostly in upper-greenschist to almandine-amphibolite facies, and the younger unit (Upper Tibestian) is a suite of quartzose sandstones, shales, and carbonate rocks in low- to upper-greenschist facies. The Lower and Upper units are apparently separated by an unconformity overlain by a thick section of conglomerate. The only available date for these metamorphic rocks is an age of about 900 Ma based on whole-rock Rb–Sr isochrons for the Lower Tibestian unit (El-Makhrouf, 1988).

The metasupracrustal rocks were intruded by calcalkaline, subduction-related, igneous suites between approximately 600 Ma and 550 Ma (Pegram et al., 1976; El-Makhrouf, 1988). These rocks are referred to as the Super-Tibestian magmatic series in the eastern part of the massif and as the Ben Ghnema batholith along the western border. The Super-Tibestian Group is not well known, but the Ben Ghnema batholith is a typical calcalkaline suite (Ghuma and Rogers, 1978; Rogers et al., 1980). It varies from dioritic and quartz dioritic rocks in the eastern part of the batholith to adamellites and granites in the west, with small bodies of gabbro scattered throughout the eastern area. Major- and trace-element concentrations show virtually identical variations to those in classic continental-margin arcs such as the Sierra Nevadas. These variations suggest that the Ben Ghnema batholith resulted from westward subduction of oceanic lithosphere beneath continental crust that presumably formed the eastern margin of the basement of the Murzuk basin. Whole-rock Rb–Sr data for different sets of samples in the major part of the Ben Ghnema batholith show ages from 550 Ma to 586 Ma, with a few pegmatitic rocks farther south yielding an age of ~533 Ma (Table 1).

Several bodies of post-orogenic to anorogenic granites were emplaced throughout the Tibesti massif during the latter stages of, or shortly following, calcalkaline activity. Very small plutons in the Eghei area are referred to as the Eghei magmatic series, which also includes a small amount of rhyolite and rhyolitic dikes (El-Makhrouf, 1988; El Makhrouf and Feiss, 1990a,b). Rb–Sr whole-rock ages range from 554 Ma to 528 Ma for the plutons and 530 Ma for dikes. A highly fractionated amazonite granite and three other alkali granites all plot near the thermal minimum in a qz-ab-Kf system. Major compositional features include $K_2O/Na_2O = \sim 1.5$; extremely low concentrations of FeO_T, MgO, and CaO; and high concentrations of LIL elements such as Rb and Ba.

The Wadi Yebigue pluton is about the same age as the Eghei magmatic series but occurs approximately in the center of the Tibesti massif (Suayah and Rogers, 1986). The pluton consists of a core of two-mica granite surrounded by a main phase that consists of biotite granite with an outer rim of biotite-hornblende granite. Despite the variation in mineralogy between different phases of the pluton, all rocks have similar compositions, including: $K_2O/Na_2O \sim 1.5$; very low concentrations of FeO_T, MgO, and CaO; and high concentrations of LIL elements. Both phases of the pluton contain accessory zircon and apatite, and the main phase also contains allanite and titanite. Modeling of whole-rock and mineral compositions shows that the two-mica and main phase granites cannot be related by addition or subtraction of minerals with the compositions that exist in the granites (Suayah and Rogers, 1986).

Vast exposures consist of unnamed granitic rocks occur throughout the Tibesti massif. Wacrenier and Vincent (1958) informally used the term "Arrye batholith"

Table 2
U–Pb isotopic data for Tibesti granites

Fraction (number of grains)	Weight (mg)[a]	Total U (ng)	Total[b] Pb (pg)	Total[b] Com. Pb (pg)	U (ppm)	Pb (ppm)	Atomic ratios								Ages (Ma)			Corr. coeff.[e]
							$^{206}Pb^{b}/^{204}Pb$	$^{206}Pb^{c}/^{208}Pb$	$^{206}Pb^{c}/^{238}U$	Error[d] (%)	$^{207}Pb^{c}/^{235}U$	Error[d] (%)	$^{207}Pb^{c}/^{206}Pb$	Error[d] (%)	$^{206}Pb/^{238}U$	$^{207}Pb/^{235}U$	$^{207}Pb/^{206}Pb$	
Hornblende granite																		
(1) HBG—Large Tip (1)	0.002	2964	277.3	1.95	1647	154	9107	0.094	0.09374	0.088	0.85817	0.109	0.06640	0.063	577.6	629.1	819.0	0.817
(2) HBG—Small prism (1)	0.002	1471	143.5	5.07	735.5	71.8	1690	0.179	0.09093	0.485	0.73658	0.508	0.05875	0.144	561.0	560.4	557.8	0.959
(3) HBG—Large prism (1)	0.002	2154	189.9	2.66	1077	94.9	4597	0.096	0.08877	0.203	0.71888	0.216	0.05873	0.074	548.3	550.0	557.2	0.940
(4) HBG—Smallest prisms (4)	0.006	1169	99.32	2.04	194.8	16.6	3197	0.075	0.08715	0.261	0.70573	0.282	0.05873	0.104	538.7	542.2	557.1	0.929
2-mica granite																		
(5) 2MG—Large equant (1)	0.002	4710	439.8	23.9	2355	219.9	1141	0.079	0.09115	0.149	0.74023	0.178	0.05890	0.095	562.3	562.5	563.4	0.846
(6) 2MG—Medium equant (1)	0.002	1986	226.9	57.9	993.2	113	206.0	0.093	0.08792	0.322	0.71384	0.385	0.05888	0.202	543.2	547.0	562.8	0.851
(7) 2MG–Tiny-StubbyPrisms (3)	0.005	2542	242.2	41.3	508.36	48.4	348.1	0.031	0.08602	0.285	0.69875	0.321	0.05892	0.142	531.9	538.0	564.0	0.897
(8) 2MG–LargeTip (1)	0.003	2917	248.3	10.7	972.4	82.8	1481	0.071	0.08525	0.281	0.69280	0.291	0.05894	0.072	527.4	534.5	564.8	0.969

[a] Weight estimated from measured grain dimensions assuming density = 4.67 g/cm^3. Uncertainty in weight is estimated to be ~20% and affects only absolute U and Pb concentrations.
[b] Corrected for fractionation (0.18 ± 0.09%/amu—Daly detector) and spike only.
[c] Corrected for fractionation, blank, and initial common Pb.
[d] Errors quoted at percent 2σ.
[e] $^{207}Pb/^{235}U$–$^{206}Pb/^{238}U$ correlation coefficient of Ludwig (1989).

Table 3
Rb–Sr and Sm–Nd data for Wadi Yebigue pluton

Sample	Rb (ppm)	Sr (ppm)	$(^{87}Rb/^{86}Sr)_p$	$(^{87}Sr/^{86}Sr)_0$	$(^{87}Sr/^{86}Sr)_i$	Sm ppm	Nd (ppm)	$^{147}Sm/^{144}Nd$	$\varepsilon_{Nd(550)}$	T_{DM} (Ga)
Main phase (biotite and biotite-hornblende) granite										
WY-46	143	92	4.503	0.7416	0.7056	9.77	54.41	0.1111	−0.47	1.11
WY-73	202	29	21.202	0.87549	0.7062	16.39	59.55	0.17025	−0.93	1.92
WY-121	137	162	2.415	0.7254	0.7061	10.93	46.07	0.14677	−0.63	1.41
WY-166	206	93	6.306	0.75727	0.7069	10.92	55.78	0.12112	−0.87	1.20
WY-176	213	59	10.526	0.78932	0.7053	11.75	50.65	0.14355	−0.95	1.40
WY-199	130	130	2.894	0.7302	0.7071	NA	NA	NA	NA	NA
Two-mica granite										
WY-182	227	49	13.534	0.81356	0.7074	2.85	10.32	0.17069	−2.22	2.17
WY-184	248	72	10.105	0.78542	0.7062	5.07	22.84	0.13727	−1.63	1.40
WY-185	246	34	21.245	0.87207	0.7055	1.85	6.76	0.16978	−1.78	2.05
WY-187	231	58	11.713	0.79838	0.7065	3.66	15.42	0.14692	−1.87	1.55

Note: Sr isotope data from Suayah and Rogers (1986); $\varepsilon_{Nd(550)}$ relative to CHUR.

for some of the rocks between the northwestern part of the Wadi Yebigue pluton and the southern part of the Ben Ghnema batholith (Fig. 1B). Unfortunately, neither the exact nature of the rock types nor the origin of any of these granitoids is known.

In contrast to both the Arabian–Nubian shield and Tuareg shield, the exposed part of the Tibesti massif shows no evidence that it consists of separate terranes assembled in the Neoproterozoic along faults, shear zones, or zones of oceanic closure. The only major fold is a Cenozoic domal uplift, which was probably also responsible for the development of small faults that cut Phanerozoic rocks and some underlying basement.

Intrusive activity in the Tibesti massif ended slightly younger than 550 Ma, and the crystalline rocks became a basement for deposition of Phanerozoic sediments. This basement is now exposed because of uplift, which may have occurred during extensive basaltic magmatism that produced large plateaus and numerous volcanic cones in several parts of North Africa during the Cenozoic (Fairhead, 1979).

4. Isotopic data for granitic rocks in the Tibesti massif

4.1. Analytical methods for new data reported in this paper

All isotopic measurements were made in the Isotope Geochemistry Laboratory of the Department of Geological Sciences at the University of North Carolina at Chapel Hill.

Ten whole-rock samples with a wide spread in Rb/Sr ratios were analyzed for Rb and Sr using a Nuclide high-resolution solid-source mass spectrometer. Samples were dissolved in a $HF–H_2SO_4$ mixture, and Rb and Sr were separated in cation exchange columns. Total procedural blanks for samples weighing a few tenths of a gram averaged 0.02 μg for Rb and 0.05 μg for Sr. $^{87}Rb/^{86}Sr$ ratios are normalized to 0.7080 for Eimer and Amend $Sr(CO)_3$. NBS 70a K-feldspar yields a $^{87}Sr/^{86}Sr$ ratio of 1.2006 ± 0.0006 (2-sigma) and $^{87}Rb/^{86}Sr$ ratio of 24.76 ± 0.38 (2-sigma).

The Rb–Sr isochron ages and initial $^{87}Sr/^{86}Sr$ ratios were calculated using a ^{87}Rb decay constant $= 1.42 \times 10^{-11}$ yr^{-1}. Errors for ages and initial $^{87}Rb/^{86}Sr$ ratios are given at 1-sigma uncertainty.

Zircon U–Pb dating was conducted on zircons separated by standard techniques including crushing, Rogers table, heavy liquids and a Frantz isodynamic separator. Zircon grains were hand picked under a binocular microscope to select grains of similar morphological types that are as clear, crack-free, and inclusion-free as possible. All zircon fractions were highly abraded to remove the outermost portions of grains that are most likely to have been affected by Pb loss.

All Pb data are reported at the 2-sigma level Total procedural blank was 96 pg Pb. Analyses were referenced to NBS 981, with $^{207}Pb/^{206}Pb = 0.9164$ and corrected by $0.086 \pm 0.009\%$/amu for fractionation. Average uncertainties (2-sigma) caused by measurement uncertainty and propagation through fractionation correction are 0.0012 for $^{206}Pb/^{204}Pb$, 0.012 for $^{207}Pb/^{204}Pb$, and 0.018 for $^{208}Pb/^{204}Pb$.

Analyses for Sm and Nd were conducted on solutions prepared by dissolving 300–500 mg of whole-rock powder in a mixture of $HF + HNO_3$. Separation of the REE group followed standard cation-exchange procedures. Sm and Nd were separated by using either HNO_3–CH_3OH on anion resin or alpha-hydroxyisobutyric acid chemistry on cation-exchange resin. Total procedure blanks were less than 1 ng for Rb and Sr and less than 500 pg for Sm and Nd.

Isotopic data for Sm and Nd were acquired on a VG Sector 54 thermal ionization mass spectrometer. Nd was analyzed in a dynamic-multicollector mode with $^{144}Nd = 1$ V (Nd+). Sm was analyzed in static-multicollector mode with $^{147}Sm = 200–500$ mV. Nd isotopic

compositions were normalized to $^{146}Nd/^{144}Nd = 0.7219$ and referenced to La Jolla $^{143}Nd/^{144}Nd = 0.511850$. External reproducibility of standards remained better than ±0.000005 (2-sigma) for Nd. Analyses of BCR–1 at the University of North Carolina using our mixed Sm/Nd tracer gave $^{143}Nd/^{144}Nd = 0.512627$, Sm = 6.581, and Nd = 28.71.

Sr_i and $\varepsilon_{Nd}(t)$ indicate initial $^{87}Sr/^{86}Sr$ and $^{143}Nd/^{144}Nd$ compositions at the crystallization age. Epsilon values for Nd relative to CHUR at the crystallization age were calculated by using $^{143}Nd/^{144}Nd_{(CHUR,0\ Ma)} = 0.512638$ and $^{147}Sm/^{144}Nd_{(CHUR,0\ Ma)} = 0.1967$. All initial ratios for the Wadi Yebigue granites were calculated for a crystallization age of 550 Ma.

4.2. Summary of new and old isotopic data available for Tibesti massif

Table 1 summarizes the limited amount of information available for initial $^{87}Sr/^{86}Sr$ ratios in the Tibesti massif. All initial $^{87}Sr/^{86}Sr$ ratios are isochron intercepts of whole-rock samples. With the exception of the Zouma amazonite granite, which clearly resulted from crustal anatexis, all granitic rocks of the massif have remarkably uniform initial $^{87}Sr/^{86}Sr$ ratios of approximately 0.706.

Four U–Pb zircon analyses from the main-phase granite consist of one multi-grain fraction and three single-grain fractions (Table 2). Two of these fractions are discordant and a third is concordant within error (Fig. 2). Regression of a line through these three points yields an upper intercept of 563 ± 3 Ma, which we interpret to represent the crystallization age of this granite. Despite fraction 1 (Table 2) being only the tip broken from a prismatic grain, it contained an inherited component that yielded a $^{207}Pb/^{206}Pb$ age of 819 Ma, and plots outside the bounds of Fig. 2.

Four U–Pb analyses from the two-mica granite consist of three single-grain fractions, including one tip broken from a large prismatic grain, and one three-grain fraction (Table 2). Because these grains all had unusually high common Pb contents and were processed at the same time as zircons from the hornblende-biotite granite (which had only 2–5 pg total common Pb, Table 2), we consider the excess common Pb to be inter-crystalline and not contamination Pb. All four analyses form a discordant trend, anchored by one nearly concordant analysis (Fig. 2) and yield an upper intercept of 557.6 ± 2.1 Ma, which we take as the crystallization age of this rock.

The only rocks analyzed for Nd isotopes are the two-mica and main-phase granites of Wadi Yebigue (Table 3). The $\varepsilon_{Nd(CHUR)}$ values relative to depleted mantle range from −1.6 to −2.2 for the two-mica granite and −0.5 to −1.0 for the main-phase granite at an age of 550 Ma (Miller and Suayah, 1994). The Sm/Nd ratios of most samples are greater than 0.23, which is higher than the mid- to upper-crustal average Sm/Nd of 0.18 (Rudnick and Fountain, 1995). Fractionation demonstrated by these high Sm/Nd ratios indicates that individual calculated T_{DM} ages are inaccurate and only suggest a Mesoproterozoic age.

Fig. 3 compares the isotopic characteristics of the Wadi Yebigue samples with granitic rocks from

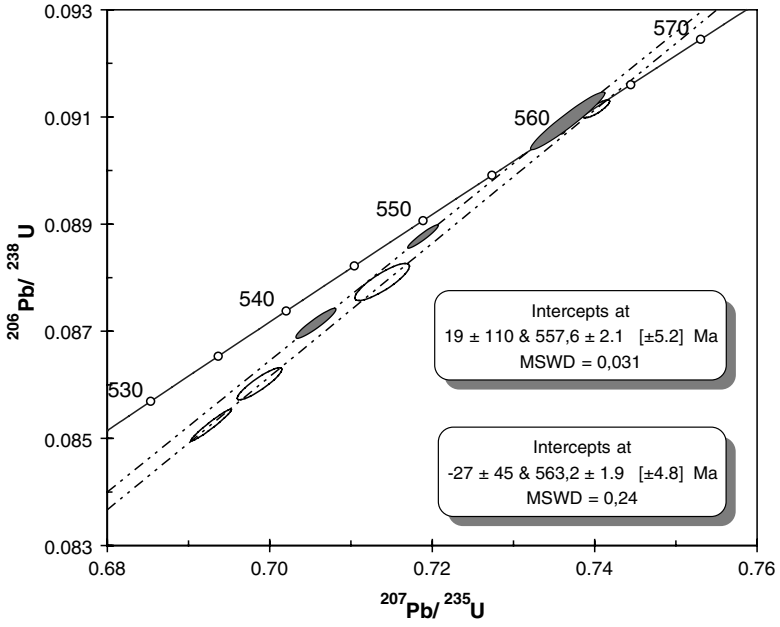

Fig. 2. U–Pb concordia diagram for Tibesti granites. Open ellipses are the two-mica granite sample, and gray shaded ellipses are hornblende granite sample. All data are reported at the 2-sigma level. Sample no. 1 in Table 2 plots outside of the area shown in this diagram.

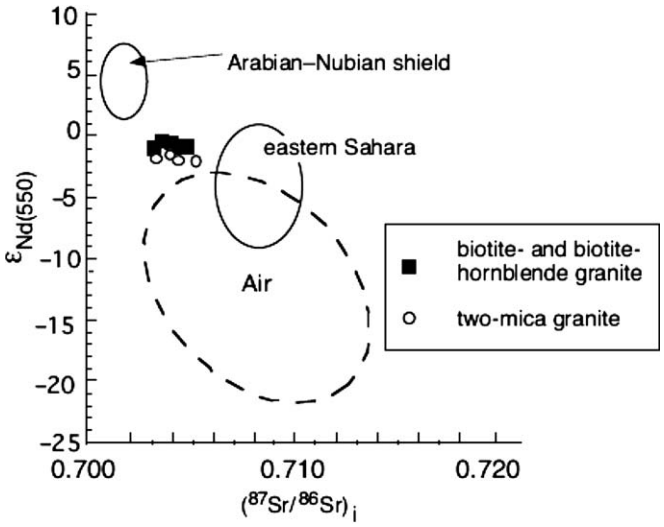

Fig. 3. Relationship between initial $^{87}Sr/^{86}Sr$ ratios and ε_{Nd} values for rocks of Wadi Yebigue (calculated at 550 Ma), Late Neoproterozoic granites in the eastern part of the Saharan region (calculated at 580 Ma; Harms et al., 1990), and Late Neoproterozoic granites and rhyolites in Air (660–600 Ma; Liegeois et al., 1994).

Precambrian exposures in the eastern Sahara and from Air. It demonstrates that granites in the Tibesti massif have isotopic compositions that show far less evidence of old continental crust than granites to the east and west.

5. Discussion and conclusions

The mechanism and time of production of magmas in the Tibesti massif must be consistent with the presence of continental crust during deposition of the metasedimentary suites that the magmas intrude. The basement for deposition of the Lower Tibestian suite is uncertain, but the Upper Tibestian was clearly deposited in a shallow-marine basin on continental crust. Sialic crust also must have been thick enough to produce conglomerates and to provide debris for extensive quartzose sandstones. Although the sediments are poorly dated, it seems likely that continental crust existed in the Tibesti area as recently as the Early Neoproterozoic and rapidly became much thinner or completely disappeared, probably because of lithospheric extension, between that time and the Late Neoproterozoic magmatic activity.

Extreme thinning of continental crust and enrichment of source regions in the Tibesti area is consistent with the concept that continental rocks existed throughout North Africa before the Late Neoproterozoic (Pan-African orogeny). Isotopic differences, however, suggest that a smaller proportion of old continental crust was incorporated in Tibesti magmas than in those in Air and the eastern Sahara region. This difference and the similarity of the Ben Ghnema batholith to granitic rocks formed by subduction along continental margins suggest that the Tibesti region was also the site of an ocean basin that had developed in the Late Neoproterozoic and closed during subduction beneath continental crust to the west.

The ocean basin may have opened and closed in a period of a few tens of millions of years within the region of older rocks apparently reworked in Late Neoproterozoic time. This possible history of the Tibesti region is similar to that of the Aracuai orogen of the Brazilian Atlantic shield in the Neoproterozoic. Pedrosa-Soares et al. (2001) described the orogen as "confined" because it opened as one arm of a rift–rift–rift triple junction and then closed back on itself between 625 and 550 Ma.

A time of ~550 Ma is about the middle of the Kuunga orogeny (Meert et al., 1995; Meert, 2003). The presence of both a short-lived ocean basin and post-orogenic granites in the Tibesti massif during the Kuunga orogeny suggests that the Tibesti Massif was in a poorly defined border region between areas of extension and post-orogenic magmatism to the east and south and the large Pharusian Ocean basin to the west.

Acknowledgements

We thank Bob Stern, A.C. Pedrosa-Soares, Randy Van Schmus, and Renaud Caby for valuable reviews of early versions of this manuscript.

References

Abdel-Fattah, M.A.-R., Doig, R., 1987. The Rb–Sr geochronological evolution of the Ras Gharib segment of the northern Nubian shield. J. Geol. Soc. Lond. 144, 577–586.

Abdelsalam, M.G., Stern, R.J., 1996. Sutures and shear zones in the Arabian–Nubian shield. J. African Earth Sci. 23, 289–310.

Abdelsalam, M.G., Liegeois, J.-P., Stern, R.J., 2002. The Saharan Metacraton. J. African Earth Sci. 34, 119–136.

Al-Saleh, A.M., Boyle, A.P., 2001. Neoproterozoic ensialic back-arc spreading in the eastern Arabian shield: geochemical evidence from the Halaban ophiolite. J. African Earth Sci. 33, 1–15.

Attoh, K., Dallmeyer, R.D., Affaton, P., 1997. Chronology of nappe assembly in the Pan-African Dahomeyide orogen, West Africa: evidence from $^{40}Ar/^{39}Ar$ mineral ages. Precamb. Res. 82, 153–171.

Black, R., Latouche, L., Liegeois, J.-P., Caby, R., Bertrand, J.M., 1994. Pan-African displaced terranes in the Tuareg shield (central Sahara). Geology 22, 641–644.

Boullier, A.-M., 1991. The Pan-African Trans-Saharan belt in the Hoggar shield (Algeria, Mali, Niger); a review. In: Dallmeyer, R.D., Lecorche, J.P. (Eds.), The West African Orogens and Circum-Atlantic Correlatives. Springer-Verlag, Berlin, pp. 85–105.

Caby, R., 1996. A review of the In Ouzzal granulitic terrane (Tuareg shield, Algeria): its significance within the Pan-African Trans-Saharan belt. J. Metam. Geol. 14, 659–666.

Caby, R., 2003. Terrane assembly and geodynamic evolution of central–western Hoggar: a synthesis. J. African Earth Sci. 37, 133–159.

Caby, R., Andreopoulos-Renaud, U., 1987. Le Hoggar oriental, bloc cratonise a 730 Ma dans la chaine pan-african du nord du continent africaine. Precamb. Res. 36, 335–344.

Caby, R., Monie, P., 2003. Neoproterozoic subductions and differential exhumation of western Hoggar (southwest Algeria): new structural, petrological, and geochronologic evidence. J. African Earth Sci. 37, 269–293.

Caby, R., Andreopoulos-Renaud, U., Pin, C., 1989. Late Proterozoic arc-continent and continent–continent collision in the pan-African trans-Saharan belt of Mali. Can. J. Earth Sci. 26, 1136–1146.

Dostal, J., Dupuy, C., Caby, R., 1994. Geochemistry of the Neoproterozoic Tilemsi belt of Iforas (Mali, Sahara): a crustal accretion of an oceanic island arc. Precamb. Res. 65, 55–69.

Duyverman, H.J., Harris, N.B.W., Hawkesworth, C.J., 1982. Crustal accretion in the Pan-African: Nd and Sr isotopic evidence from the Arabian shield. Earth Planet. Sci. Lett. 59, 315–326.

El-Makhrouf, A.A., 1988. Tectonic interpretation of Jebel Eghei area and its regional application to Tibesti orogenic belt, south-central Libya (S.P.L.A.J.). J. African Earth Sci. 7, 945–967.

El Makhrouf, A.A., Feiss, P.G., 1990a. Mineral geochemistry of three post-teconic granitic plutons, Jabal Eghei area, NE Tibesti Massif, Libya. Occasional Publication—International Center for Training and Exchanges in the Geosciences 20, 387.

El Makhrouf, A.A., Feiss, P.G., 1990b. Geology and Geochemistry of three post-tetconic granitic plutons, Jabal Eghei area, NE Tibesti Massif, Libya. Occasional Publication—International Center for Training and Exchanges in the Geosciences 20, 388.

El Makhrouf, A.A., Fullagar, P.D., 2000. The rubidium–strontium geochronology of the Pan-African post-orogenic granites of the eastern Tibesti orogenic belt, Tibesti massif, south-central Libya: application to origin and tectonic evolution. In: Sola, M.A., Worsley, D. (Eds.), Geological Exploration in Murzuk Basin. Elsevier, Amsterdam, pp. 379–395.

Fairhead, J.D., 1979. A gravity link between the domally uplifted volcanic centres of North Africa and its similarity to the East African rift system anomaly. Earth Planet. Sci. Lett. 42, 109–113.

Ghuma, M.A., Rogers, J.J.W., 1978. Geology, geochemistry, and tectonic setting of the Ben Ghnema batholith, Tibesti massif, southern Libya. Geol. Soc. Am. Bull. 89, 1351–1358.

Greenberg, J.K., 1981. Characteristics and origin of Egyptian Younger Granites. Geol. Soc. Am. Bull. 92, part 1, pp. 224–232; part. 2, pp. 749–840.

Harms, H., Schandelmeier, H., Darbyshire, D.P.F., 1990. Pan-African reworked early/middle Proterozoic crust in NE Africa west of the Nile: Nd and Sr isotopic evidence. J. Geol. Soc. Lond. 147, 859–872.

Liegeois, J.P., Black, R., Navez, J., Latouche, L., 1994. Early and late Pan-African orogenies in the Air assembly of terranes (Tuareg shield, Niger). Precamb. Res. 67, 59–88.

Ludwig, K.R., 1989. Pb-dat: a computer program for processing raw Pb–U–Th isotope data. U.S. Geol. Surv. Open File Report 88–557.

Meert, J.G., 2003. A synopsis of events related to the assembly of eastern Gondwana. Tectonophysics 362, 1–40.

Meert, J.G., Van der Voo, R., Ayub, S., 1995. Paleomagnetic investigation of the Neoproterozoic Gagwe lavas and Mbozi Complex, Tanzania, and the assembly of Gondwana. Precamb. Res. 74, 225–244.

Miller, J.S., Suayah, I.B., 1994. Pan-African magmatism and crustal growth in southern Libya: granites of the Wadi Yebigue pluton, Tibisti massif. Geol. Soc. Am. Abstracts 7, A49.

Moghazi, A.-K.M., 1999. Magma source and evolution of late Neoproterozoic granitoids in the Gabal El-Urf area, Eastern Desert, Egypt; geochemical and Sr–Nd constraints. Geol. Magazine 136, 285–300.

Muhongo, S., 1999. Geological characteristics of the suture between West and East Gondwana. Gondwana Res. 2, 595–599.

Muhongo, S., Hauzenberger, C., Sommer, H., 2003. Vestiges of the Mesoproterozoic events in the Neoproterozoic Mozambique belt: the East African perspective in the Rodinia puzzle. Gondwana Res. 6, 409–416.

Nagy, R.M., Ghuma, M.A., Rogers, J.J.W., 1976. A crustal suture and lineament in North Africa. Tectonophys. Lett. Sect. 3l, T67–T72.

Pedrosa-Soares, A.C., Noce, C.M., Wiedemann, C.M., Pinto, C.P., 2001. The Aracuai–West-Congo Orogen in Brazil: an overview of a confined orogen formed during Gondwanaland assembly. Precamb. Res. 110, 307–323.

Pegram, B.J., Register, J.K., Fullagar, P.D., Ghuma, M.A., Rogers, J.J.W., 1976. Pan-African ages from a Tibesti massif batholith, southern Libya. Earth Planet. Sci. Lett. 30, l23–l28.

Rogers, J.J.W., Hodges, K.V., Ghuma, M.A., 1980. Trace elements in continental-margin magmatism—Part II. Trace elements in Ben Ghnema batholith and nature of the Precambrian crust in central North Africa. Geol. Soc. Am. Bull. 91, part 1, pp. 445–447; part 2, pp. l742–l788.

Rudnick, R.L., Fountain, D.M., 1995. Nature and composition of the continental crust: A lower crustal perspective. Rev. Geophys. 33, 267–309.

Schandelmeier, H., Wipfler, E., Kuster, D., Sultan, M., Becker, R., Stern, R.J., Abdelsalam, M.G., 1994. Atmur–Delgo suture: A Neoproterozoic ocean basin extending into the interior of northeast Africa. Geology 22, 563–566.

Stern, R.J., 1994. Arc assembly and continental collision in the Neoproterozoic East African Orogen: Implications for the consolidation of Gondwanaland. Ann. Rev. Earth Planet. Sci. 22, 319–351.

Stern, R.J., 2002. Crustal evolution in the East African Orogen: a neodymium isotopic perspective. J. African Earth Sci. 34, 109–117.

Stern, R.J., Hedge, C.E., 1985. Geochronologic and isotopic constraints on Late Precambrian crustal evolution in the Eastern Desert of Egypt. Am. J. Sci. 285, 97–127.

Stern, R.J., Kroner, A., 1993. Late Precambrian crustal evolution in NE Sudan: isotopic and geochronologic constraints. J. Geology 101, 555–574.

Suayah, I.B., Rogers, J.J.W., 1986. Geochemistry, chronology, and petrogenesis of the Wadi Yebigue pluton, central Tibisti massif, Libya. J. African Earth Sci. 5, 413–422.

Sultan, M., Chamberlain, K.R., Bowring, S.A., Arvidson, R.E., Abuzied, H., El Kaliouby, B., 1990. Geochronologic and isotopic evidence for involvement of pre-Pan-African crust in the Nubian shield, Egypt. Geology 18, 761–764.

Toteu, S.F., VanSchmus, R.W., Penaye, J., Michard, A., 2001. New U–Pb and Sm–Nd data from north-central Cameroon and its bearing on the pre-Pan-African history of central Africa. Precamb. Res. 108, 45–73.

Toteu, S.F., Penaye, J., Djomani, Y.P., 2004. Geodynamic evolution of the Pan-African belt in central Africa with special reference to Cameroon. Can. J. Earth Sci. 41, 73–85.

Vail, J., 1985. Pan-African (late Precambrian) tectonic terrains and the reconstruction of the Arabian–Nubian shield. Geology 13, 839–842.

Wacrenier, H.H., Vincent, M., 1958. Notice explicative de la carte geologique provisoire du Borkou–Ennedi–Tibesti du 1:1,000,000: Brazzaville, Gouvernement General Afrique Equatorial Francaise, Direction des Mines et de la Geologie, 24 p.